Characterization of lacustrine harmful algal blooms using multiple biomarkers: Historical processes, driving synergy, and ecological shifts

Lin, Qi; Zhang, Ke; McGowan, Suzanne; Huang, Shixin; Xue, Qingju; Capo, Eric; Zhang, Can; Zhao, Cheng; Shen, Ji

published in
Water Research
2023

DOI (link to publisher)
10.1016/j.watres.2023.119916

document version
Peer reviewed version

Characterization of lacustrine harmful algal blooms using multiple biomarkers: Historical processes, driving synergy, and ecological shifts

Qi Lin[a], Ke Zhang[a*], Suzanne McGowan[b], Shixin Huang[a], Qingju Xue[a], Eric Capo[c], Can Zhang[a], Cheng Zhao[d], Ji Shen[a,d]

[a] State Key Laboratory of Lake Science and Environment, Nanjing Institute of Geography and Limnology, Chinese Academy of Sciences, Nanjing 210008, PR China

[b] Department of Aquatic Ecology, Netherlands Institute of Ecology, Droevendaalsesteeg 10, 6708PB Wageningen, Netherlands

[c] Department of Marine Biology, Institut de Ciències del Mar, CSIC, DC 08003 Barcelona, Spain

[d] School of Geography and Oceanography Sciences, Nanjing University, Nanjing 210023, PR China

* Correspondence:

Ke Zhang; E-mail: kzhang@niglas.ac.cn

ABSTRACT

Harmful algal blooms (HABs) producing toxic metabolites are increasingly threatening environmental and human health worldwide. Unfortunately, long-term process and mechanism triggering HABs remain largely unclear due to the scarcity of temporal monitoring. Retrospective analysis of sedimentary biomarkers using up-to-date chromatography and mass spectrometry techniques provide a potential means to reconstruct the past occurrence of HABs. By combining aliphatic hydrocarbons, photosynthetic pigments, and cyanotoxins, we quantified herein century-long changes in abundance, composition, and variability of phototrophs, particularly toxigenic algal blooms, in China's third largest freshwater Lake Taihu. Our multi-proxy limnological reconstruction revealed an abrupt ecological shift in the 1980s characterized by elevated primary production, *Microcystis*-dominated cyanobacterial blooms, and exponential microcystin production, in response to nutrient enrichment, climate change, and trophic cascades. The empirical results from ordination analysis and generalized additive models support climate warming and eutrophication synergy through nutrient recycling and their feedback through buoyant cyanobacterial proliferation, which sustain bloom-forming potential and further promote the occurrence of increasingly-toxic cyanotoxins (e.g., microcystin-LR) in Lake Taihu. Moreover, temporal variability of the lake ecosystem quantified using variance and rate of change metrics rose continuously after state change, indicating increased ecological vulnerability and declined resilience following blooms and

warming. With the persistent legacy effects of lake eutrophication, nutrient reduction efforts mitigating toxic HABs probably be overwhelmed by climate change effects, emphasizing the need for more aggressive and integrated environmental strategies.

KEYWORDS: *harmful cyanobacterial bloom; cyanotoxin; critical transition; variability; climate warming; lake paleoecology*

1. Introduction

Cultural eutrophication has resulted in a worldwide proliferation of harmful (toxic, food-web altering, hypoxia-generating) algal blooms (HABs) in freshwaters (Ho et al., 2019), threatening global water security and biodiversity (Huisman et al., 2018). In particular, the coupling of nutrient enrichment and climate warming favors cyanobacterial dominance and toxin-producing blooms which have risen through the 20th and 21st centuries (Kosten et al., 2012; Taranu et al., 2015; Kakouei et al., 2021; Meerhoff et al., 2022), with a significant occurrence of cyanotoxins in water environments (Taranu et al., 2019; Hayes et al., 2020). Management and mitigation of HABs are of tremendous concern due to their detrimental effects on ecosystem and human health (Havens and Paerl, 2015; Taranu et al., 2017). Systematic monitoring programs are typically initiated once environmental problems have emerged and they rarely capture the full spectrum of aquatic ecosystem deterioration (Battarbee et al., 2005; Qin et al., 2019). One key challenge we face, therefore, is to determine the historical baseline conditions and ecological processes (particularly decadal to centennial) of toxic cyanobacterial blooms in freshwater lakes (Huisman et al., 2018;

Ryo et al., 2019; Cao et al., 2020), and what might be the underlying mechanisms of multiple interacting drivers through time (Leavitt et al., 2009; Bruel et al., 2021; Huo et al., 2022).

Retrospective assessment using well-dated sediment archives, promisingly, provide past information on ecosystem features prior to monitoring, thus allowing reconstruction of high-resolution eco-environmental trajectories (Smol, 2010; Perga et al., 2015; Zeng et al., 2023). Traditional paleolimnological techniques for micro-algae are mostly based on microscopic identification, and use morphological remains to infer long-term changes of diatoms and a few cyanobacteria (Battarbee et al., 2005; Bunting et al., 2016). Recent advances in molecular techniques enable the analysis of sedimentary DNA to provide a broader taxonomic specificity (Monchamp et al., 2018; Cao et al., 2020; Ibrahim et al., 2020; Huo et al., 2022). Meanwhile, these techniques can be either time/labor-consuming, inadequate, or limited by undefined taphonomic and analytical issues (e.g., cumulative degradation, insufficiency of targeted reference library) (Domaizon et al., 2017). Alternatively, the rapid developments of high-performance chromatography and mass spectrometry technologies have laid a solid foundation for highly efficient and reliable approaches for analyzing multiple molecular biomarkers of photoautotrophs. In particular, a combination of aliphatic hydrocarbons (Meyers, 2003), photosynthetic pigments (Leavitt, 1993; McGowan, 2013), and cyanotoxins (Henao et al., 2019) applied to lake sediments can achieve unprecedented information on past dynamics of primary producer communities (e.g. phytoplankton versus macrophyte dominance), HABs, and toxin production (Waters

et al., 2021).

Impacts of multiple stressors on freshwater ecosystems, such as climate change, eutrophication, hydrological alterations, and trophic cascades, may (i) complicate the identification of drivers and their interactions that are responsible for key changes (Leavitt et al., 2009; Deng et al., 2014), (ii) increase the risk of catastrophic shifts (e.g., macrophyte extinction, HABs) (Scheffer et al., 2001), and (iii) compromise the potency of restoration measures by changing the baseline conditions (Battarbee et al., 2005; Bruel et al., 2021). In lake ecosystems, temporal variability in primary production can rise due to persistent increases in nutrient influx (e.g., the paradox of enrichment) (Cottingham et al., 2000; Bunting et al., 2016), after which the state shift to prolific cyanobacteria is triggered by relative minor forcing (eg., warming) that push lakes beyond critical thresholds (Dakos et al., 2015). The complexity and interactivity of stressors on ecosystems further hamper our understanding of how reducing local pressures may increase ecosystem resilience to climate change (Monchamp et al., 2018; Bruel et al., 2021; Carpenter et al., 2022). Retrospective examination of past ecological shifts and variability characteristics using long-term records, therefore, may provide critical insights on how nonlinear and abrupt HABs in response to environmental change may improve lake management and mitigation strategies (Bunting et al., 2016; Ryo et al., 2019; Bjorndahl et al., 2022).

In this study, we quantified one-century long changes in the production, composition, variance, and rate of change of phototrophic assemblages, particularly toxigenic cyanobacteria and their toxic metabolites, in a typical eutrophic lake (Lake

Taihu, China) suffering from increasingly frequent cyanobacterial HABs. High-resolution time series of sedimentary biomarkers (*n*-alkanes, chlorophyll and carotenoid pigments, microcystins) and geochemistry (organic carbon, nutrients, metals) were quantitatively integrated with monitoring data and historical archives using ordination analysis and generalized additive models. We address two key questions: (i) what are the dynamic trajectories of photoautotrophic succession (macrophyte versus phytoplankton), HABs, and cyanotoxin production, and how were catastrophic shifts shaped by multiple stressors interacting through time? (ii) whether current HABs and historical changes in ecological variability were consistent with the establishment of an alternative stable state in Lake Taihu, and what are the implications for ecosystem resilience and baselines? Our methodology has considerable potential application globally to provide evolutionary insights into the mechanisms of freshwater ecosystem degradation and to open new management perspectives for ecological adaptation (Perga et al., 2015) to climate warming.

2. Materials and methods

2.1. Study area and sampling

Lake Taihu, China's third largest freshwater lake (~2,338 km^2), is located in the rapidly developing and highly urbanized Yangtze River Delta (Fig. S1). Currently, the catchment area is dominated by agricultural land (47.9%), urban land (24.3%), and water bodies (13.6%) that supports 4.8% (~65 million) of China's population and produces 11.6% of national GDP, despite occupying only 0.4% (~36,500 km^2) of

China's land area. There are approximately 219 rivers, with inflows going to the northern and western lake sides, and outflows occurring on the eastern sides. Due to nutrient supply and climate warming, this shallow (<3 m) lake has experienced accelerated eutrophication accompanied by potentially toxic cyanobacterial blooms (*Microcystis* spp.) (Guo et al., 2019). Coupled with southerly or southeasterly winds, annual cyanobacterial HABs occur earlier and persist longer in the northern and western lake (Shi et al., 2019), threatening the water security of approximately 30 millions of inhabitants (Qin et al., 2019). However, continuous water quality monitoring and remote sensing observations are limited to recent ~30 years.

In order to reconstruct longer-term history of lake eutrophication and HABs for assessing ecosystem state dynamics and optimizing management strategies, two duplicate sediment cores (~40 cm) with intact sediment-water interfaces were retrieved (Smol, 2010) from one typical, relatively sedimentation-stable area of Lake Taihu (central west, N31.11623°, E120.06152°) in March 2017 and July 2020 (Fig. S1) (Lin et al., 2020). The cores were cut into 0.5-cm contiguous intervals, and subsamples were refrigerated at –4 ℃. Modern samples including cultured cyanobacterium *Microcystis* (n=5), predominant macrophytes (6 species), and surface forest soil (n=5) in and around the lake were also collected (Table S1). In the laboratory, all the samples were freeze-dried, and core sediment subsamples were processed for radiochronology, physicochemical parameters, and biomarker analyses. The sediment core collected in 2020 was specifically for the measurement of microcystins, and other proxy analyses were conducted on the previous core. These

147 cores from the increasingly blooming area were taken as an analytical test for
148 multi-biomarker reconstruction in this study.

149 ## 2.2. Radiochronology

150 Isotopes of ^{210}Pb, ^{226}Ra and ^{137}Cs for sediment dating were measured using a
151 gamma spectrometer (ORTEC., USA), which provides an absolute detection
152 efficiency (≥95%) according to calibrated sources and standard samples. The age
153 model of the sediment core collected in 2017 was computed with *serac* R package
154 (Bruel and Sabatier, 2020). We have previously reported detailed protocols of
155 geochronology and reliable results that suggested mean sedimentation rates of 0.38
156 cm yr^{-1} for the lake area over the past hundred years (Lin et al., 2020). The age for
157 another core was thus determined through core matching based on lithology and
158 gecochemical parameters (Cheng et al., 2023).

159 ## 2.3. Sediment physicochemical analysis

160 The analytical determination of major sediment physicochemical parameters,
161 including grain size, mass magnetic susceptibility, metal elements (e.g., Al, Ti, Fe,
162 Mn), total phosphorus (P), total nitrogen (N), organic carbon (OC), and nutrient
163 stoichiometry (molar ratios of C/N and N/P) have been well described in our previous
164 studies (Lin et al., 2020, 2021). The temporal changes of these paleovariables are
165 shown in detail in Fig. S2.

166 ## 2.4. Multi-biomarker analysis

167 Three kinds of sedimentary molecular biomarkers were analyzed

comprehensively in Lake Taihu cores to characterize the integral historical processes of HABs. First, aliphatic hydrocarbons (particularly *n*-alkanes) were used to distinguish the relative contributions of organic matter from algae, macrophytes, and terrestrial plants, reflecting major succession of photoautotrophic communities (Meyers, 2003). Second, photosynthetic subfossil pigments are reliable indicators to track the past changes in lake primary productivity and algal community (McGowan, 2013), particularly the abundance and composition of bloom-forming algae (Bjorndahl et al., 2022). On this basis, concentrations of cyanotoxins were measured in the sediments to infer the magnitude of past HABs and their toxin production through time (Waters et al., 2021).

Aliphatic hydrocarbons. Sediment core subsamples, samples of cultured cyanobacterium *Microcystis*, collected aquatic macrophytes, and surface forest soil were all analyzed for *n*-alkanes following standard procedures (Zhang et al., 2019). In brief, homogenized dry samples were ultrasonically extracted four times using the dichloromethane/methanol (9:1, v/v) mixture. Total lipids were concentrated to dry with pure nitrogen and saponified with 6% KOH in methanol at room temperature for 12 h. The neutral lipids containing *n*-alkanes were further extracted with n-hexane through silica gel column chromatography. Finally, *n*-alkanes were measured using an Agilent 7890 Gas Chromatograph (GC) equipped with an Agilent 5975 mass spectrometer (MS) with an external C16 standard for identification and quantification. A set of proxies (ACL, TAR, P_{aq}, and S/M) were calculated based on odd-carbon *n*-alkanes to identify the composition and sources of sedimentary organic matter

(Ficken et al., 2000; Meyers, 2003), which are explicitly described in the Supporting Information (Text S1).

Photosynthetic subfossil pigments. Sedimentary chlorophyll and carotenoid pigments were extracted and purified following the standard method with optimal mixtures of acetone, methanol, and deionized water at –20 ℃ for 12 h (McGowan, 2013). After filtering, nitrogen blowing, and re-dissolution, individual chlorophyll and carotenoid compounds were isolated and quantified using an Agilent 1200 series high-performance liquid chromatography unit (HPLC, Canada) with an ODS Hypersil column (250×4.6 mm; 5 μm particle size) and photo-diode array detector. Pigment concentrations were calibrated with authentic standards (DHI Lab, Denmark) and are expressed as nmol pigment g^{-1} OC because the degradation of organic pool can partly compensate for bias of pigment diagenesis (Leavitt, 1993; McGowan, 2013). An ultraviolet radiation (UVR) index was calculated by dividing UVR-absorbing pigment (scytonemin derivative) relative to the sum of key carotenoids (diatoxanthin, lutein-zeaxanthin, and alloxanthin) and multiplying by 100 (Leavitt et al., 1997). Calibration in whole-lake experiments revealed that this index increases as a linear function of the depth of UVR penetration (Leavitt et al., 1997), such that higher index values indicate greater exposure to potentially damaging UVR, namely better light conditions and higher water clarity (McGowan et al., 2012).

Cyanotoxins. Sedimentary microcystins (MCs) were analyzed following previously published procedures (Cheng et al., 2023). Briefly, homogenized sediment subsamples were ultrasonically extracted three times using 0.1 mol EDTA/$Na_4P_2O_7$

(1:1, v/v, pH=3) mixture. The extracts were loaded into hydrophilic-lipophilic balance cartridges previously activated with methanol and washed with deionized water. After a further washing step and elution with methanol, the toxin eluent was dried using pure nitrogen at 40 ℃. Finally, three dominant MC congeners (MC-LR, MC-YR, MC-RR) (Henao et al., 2019; Xue at al., 2023) were measured using a Waters H-class ultra HPLC tandem triple quadrupole mass spectrometer (USA) with an Acquity UPLC BEH C18 column (100×1 mm, 1.7 μm particle size). The calibration ranges were 0–200 μg L^{-1} ($R^2 \geq 0.99$) using MC standards from Sigma-Aldrich (≥95%, Germany), and the relative standard deviations were less than 5% as quantified from external standards and blanks. The MCs were reported as ng toxin g^{-1} OC to compensate for diagenetic degradation (Waters et al., 2021).

2.5. Historical data

Time series of major environmental variables from the study area were collected for the past ~120 years to quantify the statistical relationships between the paleorecords of lake ecosystem status (*n*-alkanes, pigments, cyanotoxins, OC, total nitrogen and phosphorus) and identify potential causal effects associated with regional changes in climate, agriculture, and urbanization (Fig. S3). Climate records including annual mean air temperature, wind speed, and total precipitation were obtained from a nearby meteorological station #58358 of China (https://data.cma.cn/) with supplements from the global historical climatology network (https://cdiac.ornl.gov/). Estimates of agricultural intensity referring to total fertilizer and pesticide consumption and rice yield (Bunting et al., 2016) were compiled from official

234 statistical data of nearby cities (https://www.stats.gov.cn/) and previous documents
235 (Ellis and Wang, 1997). Historical records of urbanization (mainly urban sewage) as
236 mirrored by total wastewater effluent, local population (dominated by urban
237 inhabitants) and GDP (McGowan et al., 2012) were obtained from Taihu Basin
238 Authority of Ministry of Water Resources and official statistical documents (Fig. S3).
239 Although too short for our statistical analysis, limnological variables monitored
240 during 2005–2020 were obtained from the Taihu Laboratory for Lake Ecosystem
241 Research for data integration.

242 **2.6. Numerical analysis**

243 Temporal variations of historical document data, lake geochemical variables and
244 biomarkers were visualized using Grapher 14 and R software. Sedimentary
245 paleorecord time series (*n*-alkanes, pigments, total MCs, OC, nitrogen, and
246 phosphorus) were log-transformed if needed, then centered (mean=0), standardized
247 (variance=1.0), and harmonized to equivalent sampling intervals prior to statistical
248 analyses (Bunting et al., 2016).

249 *Change phase analysis.* The timings of paleorecord changes were determined
250 using stratigraphically constrained incremental sum of squares (CONISS) cluster
251 analysis in the Tilia program. Sequential T-test algorithm based on variance analysis
252 with prewhitening (p<0.05, cut-off length=10) and calculation of cumulative sum of
253 differences were also performed to identify significant change points and the main
254 phases of past ecological dynamics (Andersen et al., 2009; Cao et al., 2020).

255 *Ordination analysis.* The gradient length of <1 total standard deviation unit for

the paleorecords suggested that a linear model was suitable for unconstrained and constrained ordinations using Canoco 5 program (ter Braak and Šmilauer, 2012). Nonmetric multidimensional scaling (NMDS) analysis based on Bray–Curtis distances was performed to identify structural changes in paleorecords through time in a reduced two-dimensional space. For technical purposes, the scores of both NMDS axes (NMDS1, NMDS2) were taken as the main representative variation indices of ecological dynamics (Ibrahim et al., 2020). Up to ten environmental variables referring to regional climate, agriculture, and urbanization (Fig. S3) were included in the initial analysis to evaluate their significance and collinearity, via a series of forward selection and restricted Monte Carlo permutation tests (n = 999) (ter Braak and Šmilauer, 2012). Four runs of redundancy analysis (RDA) were then conducted to explore potential relationships between paleorecords and individual categories of significant environmental variables of agriculture (fertilizer consumption), urbanization sewage (population), and climate (air temperature, wind speed), respectively. Variance partitioning analysis (VPA) was used to estimate the fractions of historical variances in the paleorecord time series explained by all categories of significant environmental variables and their interactions (Bunting et al., 2016).

Generalized additive model analysis. Generalized additive models (GAMs) analysis were performed to distinguish and quantify the impacts of local human activity and regional climate change on Lake Taihu ecosystem dynamics through time. The inferred human index (i.e., weighted averages of z-score normalized population and fertilizer consumption) and climate index (i.e., ratios of annual mean air

278 temperature to wind speed) were chosen as representative predictor variables, while
279 the response variables were scores of both NMDS axes calculated from the dataset
280 collating multiple paleorecords (details in Text S2). The functions *gam* and
281 *predict.gam* from "mgcv" package in R software (Wood, 2017) were used, and GAMs
282 analyses were conducted following standard procedures (Simpson, 2018) and our
283 previous descriptions (Lin et al., 2021).

284 *Temporal variability analysis.* Sedimentary pigments and other biomarkers can
285 accurately record the variability of algal communities following fertilization through
286 time (Cottingham et al., 2000; Meyers, 2003), and thus reliably reflect changes in
287 ecosystem variability during state shifts (Carpenter et al., 2011; Bunting et al., 2016).
288 Historical changes in the temporal variability of total autotrophic production (Chl *a* +
289 echinenone), bloom-forming algal abundance (sum of canthaxanthin and
290 lutein-zeaxanthin) (Bunting et al., 2016; Bjorndahl et al., 2022), cyanotoxins (total
291 MCs) (Waters et al., 2021), and the scores representing paleorecord structure
292 (NMDS1) were estimated by the numerical simulation of both variance and rate of
293 change (RoC) following standard technical recommendations (Simpson, 2018;
294 Bjorndahl et al., 2022). The variances were extracted by calculating the standard
295 deviations performed with the "earlywarnings" packages in R (Dakos et al., 2015).
296 The RoCs were generated from the posterior simulations of the fitted GAMs using the
297 first derivative of a spline. All models fitting the selected time series contained a
298 continuous-time first-order autoregressive [CAR(1)] process to account for temporal
299 autocorrelation. These analyses were performed using R software with the "mgcv"

300 and “vegan” packages (Wood, 2017; Simpson, 2018).

301 3. Results

302 Multiple analyses of sediment cores from Lake Taihu revealed distinct dynamics
303 of lake primary producers following fertilization and climate change. Proxies for
304 organic matter, nutrients, autotrophic production, and cyanobacterial HABs showed
305 particularly prominent changes, which exhibited three similar phases since the 1900s.

306 3.1. Sedimentary OC, nutrients and *n*-alkanes

307 Sediments were mainly composed of coarse silt (16–63 μm), accounting
308 for >50% prior to 1950. Peaks of OC, C/N ratios (>12), total phosphorus and nitrogen
309 in the mid-1910s and -1930s, coeval with higher sand content and lithogenic elements
310 (e.g., Al, Ti) (Fig. 1A and Fig. S2), probably showed enhanced inputs of terrigenous
311 nutrients and organic matter (Meyers, 2003). Sedimentary *n*-alkanes before the 1950s
312 were dominated by middle-chain (*n*-C_{21}, *n*-C_{23}, *n*-C_{25}) and long-chain (*n*-C_{27}, *n*-C_{29},
313 *n*-C_{31}, *n*-C_{33}) components (averaged 87.5%) (Fig. 1A and Fig. S4) similar to that of
314 macrophytes and surface soil (Fig. S5). These characteristics together with relatively
315 high values of TAR and P_{aq} (>0.4), and low S/M ratios suggested dominant
316 contributions of organic matter from submerged/floating macrophytes and
317 allochthonous origin (Ficken et al., 2000; Meyers, 2003).

318 During the 1950s–1980s, content of fine silt (4–16 μm) and lithogenic elements
319 increased slightly while OC and nutrients remained stable (Fig. 1A and Fig. S2). The
320 C/N ratios decreased continuously to <10 and proportions of short-chain *n*-alkanes

(n-C_{17}, n-C_{19}) increased sharply since the mid-1970s, reflecting substantially higher algal organic matter contribution, as algal communities (particularly cyanobacteria) have been identified as main contributors of short-chain *n*-alkanes in our survey (Fig. S5) and previous analyses (Zhang et al., 2017). Middle-chain *n*-alkanes and P_{aq} decreased and remained at low levels while S/M ratios fluctuated and increased to a high level, suggesting a potential transition toward an algae-dominated lake state. Meanwhile, long-chain *n*-alkanes, ACL, and TAR as indicators of allochthonous organic matter input (Meyers, 2003) showed coeval decreases and relatively low values from ~1970.

Since the 1990s, sediments were dominated by fine particles (<16 μm) enriched with magnetic mineral and lithogenic elements (Fig. S2) relating to well-weathered terrigenous detritus (Lin et al., 2020). Sedimentary phosphorus, nitrogen, and OC showed ~1.5-fold increases while C/N ratios fluctuated around 10. Short-chain *n*-alkanes from algae maintained a relatively high abundance followed by a decrease, whereas middle-chain *n*-alkanes and P_{aq} values remained relatively low and stable (Fig. 1A). These results along with relatively high S/M ratios suggested an algae-dominated organic matter source and a lake ecological regime that has greatly deviated from the historical conditions prior to 1950.

3.2. Subfossil pigments and cyanotoxins

Analyses of subfossil chlorophylls, carotenoids, and cyanotoxins revealed main shifts of algal communities are consistent with pronounced lake eutrophication (Figs. 1B and 2). An increase in the ratios of labile to chemically-stable chlorophylls (Chl *a* :

343 Pheophytin *a*) in the upper core (Fig. S6) reflected slightly improved pigment
344 preservation when algal production increases as expected (Leavitt, 1993; Waters et al.,
345 2021). Additionally, ratios of total carotenoids to total identified pigments did not
346 change with depth, indicating a relatively constant preservation environment since the
347 1900s. This phenomenon coincided with generally stable redox conditions since the
348 1950s as inferred from Fe/Mn ratios (Fig. 2). Thus, the molecular biomarkers were
349 well-preserved in recent sediments of Lake Taihu beyond similar human-impacted
350 waters elsewhere (Bunting et al., 2016; Zastepa et al., 2017; Waters et al., 2021;
351 Huang et al., 2022; Zeng et al., 2023).

352 Cluster analysis of pigment assemblages identified the most significant turning
353 points around the 1950s and 1980s, and that algal communities showed two main
354 patterns of change (Fig. 1B). First, concentrations of pigments from siliceous algae
355 (diatoxanthin) and cryptophytes (alloxanthin) that commonly grow in the spring
356 (Deng et al., 2014), were too low to be detected before ~1995, then generally
357 increased in recent sediments. Second, subfossil biomarkers from summer
358 bloom-forming colonial cyanobacteria and chlorophytes (canthaxanthin,
359 lutein-zeaxanthin, pheophytin *b* and *b′*) (Guo et al., 2019), together with
360 chemically-stable indicators of total algal abundance (*β*-carotene, total carotenoids),
361 were relatively constant during most of the 20th century, increased 300–700% to high
362 levels during the 1980s–1990s, then showed few fluctuations or lower trends in the
363 recent decade. The echinenone (cyanobacterial pigment) that is often found to be
364 extremely enriched in *Microcystis* (Hesse et al., 2001) was coeluted with labile Chl *a*

365 (all phototrophs) in HPLC, which collectively showed a ~9-fold increase similar to
366 *β*-carotene. Correspondingly, a sharp decrease of the UVR index occurred during the
367 1980s–2000s, indicating a marked decline in UV exposure and water clarity (Leavitt
368 et al., 1997). Taken together, these results demonstrate that algal production increased
369 ~3- to 7-fold since the 1980s when an ecosystem state shift was initiated. Recent
370 modification of algal communities inferred from pigments is basically consistent with
371 modern monitoring and molecular genetic results that showed a >50% phytoplankton
372 biomass contribution from *Microcystis*-dominated cyanobacteria (Zhang et al., 2018a;
373 Guo et al., 2019; Zhang et al., 2023).

374 Cyanotoxins (three microcystin congeners) were detected throughout the
375 century-long sediment record, and their production showed historical variations
376 corresponding to bloom-forming cyanobacterial proliferation (Fig. 2). In general,
377 concentrations of total MCs fluctuated without clear directional trends before ~1950,
378 peaked between the 1960s (514 ng g^{-1} OC) and the 1980s (1,752 ng g^{-1} OC), then
379 increased exponentially since the 1990s to the highest value (~40,000 ng g^{-1} OC) in
380 the surface sediments. Elevated production of total MCs was mainly sourced from
381 increased contributions of highly toxic MC-YR (averaged 45%) and MC-LR
382 (averaged 36%), whereas contribution of hypotoxic MC-RR (averaged 19%)
383 generally decreased since the 1950s. Moreover, rapid growth of cyanotoxin
384 production was in pace with enriched nitrogen, phosphorus, elevated N/P ratios, and
385 decreased C/N ratios, indicating a combined effect of nutrient inputs and
386 stoichiometry changes (Xue at al., 2023).

3.3. Driver-response relationships

NMDS analysis tracked three distinguishable groups from biomarker and geochemistry assemblages since the 1900s (Fig. S7), as also observed from the stratigraphic temporal cluster (Fig. 1). The main gradient of paleorecord changes was associated with increased levels of autotrophic production, bloom-forming cyanobacterial proliferation, cyanotoxin occurrence, and loss of macrophytes and water clarity as nutrient enrichment led to changes in trophic state. This ecological gradient was highly correlated with NMDS1 and explained 81.3% of variation compared to 18.7% from NMDS2. Further statistical analyses using sequential T-test and cumulative sum of differences for NMDS1 scores confirmed shifting points of the lake ecosystem around the 1950s and 1980s (Fig. S8).

RDA with the agriculture predictor (fertilizer) alone explained 32.1% of variation in geochemistry and biomarkers during the past hundred years, similar to the variation explained by the sewage predictor (population, 30.9%) alone (Fig. 3A and Fig. S9). In contrast, RDA using climate variables either elevated air temperature (23.6%) or declined wind speed (30.6%) alone explained fewer changes in the paleorecords. VPA showed that environmental variation associated with agriculture, sewage, and climate totally explained 61.4% of past dynamics in lake ecosystem (Fig. S9). Comparison of individual and interactive categories suggested that most of the explained variance arose from total interactions between agriculture, sewage, and climate change (20.1%), followed by that from sewage (17.5%) and that from agriculture (10.4%) alone (Fig. 3A). The remaining unexplained variance (38.6%)

409 may be related to other environmental factors, particularly precipitation, hydrological
410 fluctuations, and extreme weather events, which are important but usually hard to
411 statistically quantify in long-term driver-response analysis (McGowan et al., 2012;
412 Bunting et al., 2016).

413 GAMs estimated when and to what extent human activities and climate change
414 contributed to the past ecological dynamics of Lake Taihu, as indicated by the
415 NMDS1 and NMDS2 scores of the paleorecords (Fig. 3). Documentary data-inferred
416 human and climate indices (Text S2, Fig. S7) were considered as representative
417 predictor variables according to our RDA results and previous investigations at Lake
418 Taihu (Zhang et al., 2018b; Lin et al., 2021). Human and climate indices together
419 explained 94.4% of variation in NMDS1 and 91.3% in NMDS2, respectively (Table
420 S2). The smooth functions (Fig. 3B) illustrated a nonlinear response of NMDS1 to
421 human index and a significantly linear response to climate. NMDS2 also responded
422 significantly to human and climate indices with nonlinear trends. From a temporal
423 perspective, the simultaneous effects of changing human activity and climate were
424 detected for both NMDS axis scores since the 1980s when simultaneous positive
425 effects on the NMDS1 prevailed (Fig. 3C). As lake trophic status deteriorated, the
426 contribution of climate increased and even surpassed that of anthropogenic nutrient
427 influx in recent decades.

428 **3.4. Historical changes in ecological variability**

429 The fitted GAMs were significant (p<0.001) for dominant biomarker time series
430 of primary producers, community turnover, and cyanotoxins (Table S3), allowing

estimation of historical patterns of lake ecosystem variability. Temporal trends in variance and RoC were similar for specific variables (Fig. 4A). Variance of time series in total and bloom-forming algae (particularly cyanobacteria) started to increase from the early 1990s, and the corresponding RoCs increased significantly since the mid-1980s. In contrast, cyanotoxins showed sharp increases in variance and RoC after ~2010, lagging behind the initial *Microcystis* blooms. Changes in variance and RoC of the scores of NMDS1 axis were particularly coherent in recent three decades, manifesting as a significant increase followed by a decline. Notably, temporal variability of these key ecosystem components increased to varying degrees following the apparent ecosystem state change.

4. Discussion

This work shows that integrated application of multi-biomarkers and geochemistry proxies on lake sediment sequences provides a powerful means to retrospectively assess long-term dynamics in HABs, cyanotoxin production, and ecosystem variability in response to multiple stressors and their interactions. Our results revealed critical processes of eutrophication and primary production culminating in an abrupt ecological shift, characterized by increasingly-toxic cyanobacterial blooms (*Microcystis*) from the 1980s in Lake Taihu. Thereafter increasing ecological variability suggested that Lake Taihu was probably subjected to elevated variation in the forcing mechanism (Dakos et al., 2015), and/or exhibited a paradox of enrichment (Cottingham et al., 2000; Bunting et al., 2016) with nutrient

cyclic loops (Scheffer et al., 2001; Xu et al., 2021), which failed to establish an alternative stable state (Carpenter et al., 2011). Our findings have demonstrated increased ecological vulnerability and reduced predictability of cyanobacterial HABs following state change and climate warming, which has profound environmental implications.

4.1. Multiple stressors underlying HABs and cyanotoxin production

Freshwater ecosystems are widely experiencing the "allied attack" of climate change and eutrophication (Moss et al., 2011), particularly for degrading shallow lakes (Zhou et al., 2022), given their potential driving synergy (Paerl and Scott, 2010; Meerhoff et al., 2022). As shown in previous investigations (Kosten et al., 2012), experiments (Richardson et al., 2019), modelling (Taranu et al., 2017; Kakouei et al., 2021), and syntheses (Havens and Paerl, 2015; Taranu et al., 2015; Jeppesen et al., 2020), eutrophic conditions and warmer climate contribute to higher phytoplankton biomass and cyanobacterial dominance, thus increase the risk of toxic HABs and water quality degradation (Huisman et al., 2018). This phenomenon is extremely true for large, shallow Lake Taihu, similar to lakes Okeechobee (USA), Winnipeg (Canada), Võrtsjärv (Estonia), Kasumigaura (Japan), Chaohu (China), and shallow parts of other large lakes worldwide (Qin et al., 2019; Zhou et al., 2022). Accelerated climate warming and nutrients influx (N, P) from the watershed due to rapid agricultural expansion and urbanization (Fig. S3) are widely recognized as the driving factors (Xu et al., 2021; Zeng et al., 2023). Our paleolimnological reconstruction and ordination results (Figs. 2 and 3A) offered empirical complement of lake

474 eutrophication from long-term perspective, associating largely with agricultural
475 practices and urban sewage.

476 Moreover, interactions between climate change (warming, wind stilling) and
477 anthropogenic nutrients in VPA explained a large part of the historical dynamics in the
478 Taihu ecosystem (Fig. 3A). This is consistent with theoretical and empirical
479 expectations that environmental effects work on lakes via coupled influxes of energy
480 (temperature, irradiance, wind) and mass (precipitation, nutrients, particles) (Leavitt
481 et al., 2009). According to the GAM results (Fig. 3C), the majority of the forcing
482 interactions through time were cumulative with simultaneous positive effects since
483 intensified fertilization and cyanobacterial blooms in the 1980s. Thus, our empirical
484 results highlight the synergistic effects of eutrophication and climate change on
485 cyanobacterial temporal dynamics.

486 As previously and newly-loaded nutrients are effectively retained and recycled in
487 Lake Taihu (Zhu et al., 2020; Xu et al., 2021), warming effects have produced a suite
488 of favorable environmental conditions to sustain the HAB potential. First,
489 phytoplankton universally optimize growth as temperatures increase to a certain
490 extent, notably for cyanobacteria and other bloom-forming algae that prefer warming
491 conditions (Carey et al., 2012; Havens and Paerl, 2015). Second, enhanced water
492 column stability and thermal stratification following joint regional warming and
493 atmospheric stilling (Fig. S3) modify phytoplankton communities by favoring surface
494 bloom-forming cyanobacteria through buoyancy regulation (Kosten et al., 2012). The
495 consequent accumulation of detrital organic matter from algae in summer and autumn

usually enhances deoxygenation of subsurface water layers, stimulates the release of internal phosphorus (Yin et al., 2022), and inhibits nitrification-denitrification coupling in Lake Taihu (Zhu et al., 2020). This is also indicated by the shifts in the sediment nutrient stoichiometry, such as elevated N/P ratios and fluctuated C/N ratios following blooms (Fig. 2). Bloom-induced underwater light attenuation (Fig. 1B) further reinforce buoyant cyanobacteria dominance (Carey et al., 2012; Guo et al., 2019). Third, rising temperature can not only increase the mineralization rate of watershed soils, but also be accompanied by more extreme rainstorms, both of which could enhance diffuse and legacy nutrient delivery to waters. Tropical cyclones and extreme weather have been reported to play an important role in stimulating cyanobacterial bloom formation in Lake Taihu (Zhu et al., 2014; Yang et al., 2016). Furthermore, human and climate-driven hydrological alterations (e.g., ~20% rise of Taihu lake-level since 1992) (Zhang et al., 2018b), combined with projected warming and drought (Woolway et al., 2020), are expected to extend vertical stratification and water residence time, which will likely promote HABs and complicate eutrophication management (Havens and Paerl, 2015; Yang et al., 2017; Meerhoff et al., 2022).

In turn, the interactive effects also strongly stimulate the production of hazardous cyanotoxins, particularly microcystins, as found in microcosm experiments (Lürling et al., 2018). Our biomarker reconstruction revealed that significant increases in MCs lagged behind the initial blooms by over a decade in Lake Taihu (Fig. 2), until the shift to and formation of toxic *Microcystis* blooms (Hu et al., 2016; Guo et al., 2019) as climate change and eutrophication intensified in the 1990s. In particular, this

process promoted the strains producing more toxic MC-LR and MC-YR and exacerbated the ecological risk, as similarly observed in other degraded freshwaters (Zastepa et al., 2017; Henao et al., 2019). Increasing temperature and nutrient concentrations are corroborated as major predictors of large increases in regional MC maxima (e.g., North America) (Taranu et al., 2017; Hayes et al., 2020) and even global patterns of MC congeners (Taranu et al., 2019). Despite faster photodegradation in some environments (e.g., the tropics), surface freshwaters like Lake Taihu in the warming future might experience a predicted higher occurrence of highly-toxic MCs, with increasing risks to environmental and human health.

Multiple stressors can further provoke large changes in food webs with potential cascading effects, in particular weakening top-down control in regulating phytoplankton biomass and HABs (Meerhoff et al., 2022). In Lake Taihu, long-term loss of macrophytes (Fig. 1A) probably have caused less refuge available for phytoplankton competitors, such as grazer macroinvertebrates and zooplankton (Moss et al., 2011; Janssen et al., 2014). Over-fishing and extensive stocking have altered lake fish community diversity and structure by favoring large amounts of small zooplanktivorous species (notably anchovy) (Mao et al., 2020). These shifts in aquatic communities substantially reduced algal grazing by zooplankton in the lake. Furthermore, fewer piscivorous fish, more omnivorous and herbivorous species, and decreased body size of zooplankton are expected in warmer waters (Jeppesen et al., 2020). Such changes are likely to reinforce the positive interaction between climate change and eutrophication, given the projected algal proliferation, toxin-producing

cyanobacterial dominance, and less intensive top-down effects.

4.2. Ecosystem state shift and baseline implications

Studies on shallow lakes suggest that increased variations in phytoplankton parameters and regulatory mechanisms are reliable indicators of ecosystem state change from clear-water to turbid-water dominated by prolific, nuisance cyanobacteria (Scheffer et al., 2001; Janssen et al., 2014; Yang et al., 2017). This catastrophic shift may arise from abrupt but persistent changes in external forcing (e.g., climate change, nutrient enrichment) and/or gradual variation in intrinsic factors (e.g., trophic cascades) (Bunting et al., 2016; Carpenter et al., 2022). Ecological theory predicts that during the transitions among alternate stable states, lake ecosystems may exhibit transient (rising then decreasing) variability in focal parameters (Carpenter et al., 2011; Dakos et al., 2015) following the re-establishment of internal feedback mechanisms (e.g., internal nutrient cycling, loss of macrophytes, shading) (Scheffer and van Nes 2007; Janssen et al., 2014). However, both temporal variance and RoC analyses in Lake Taihu explicitly demonstrated increasing phytoplankton variability after the ecological shift (Fig. S8 and Fig. 4A), suggesting that a stable state has not yet been established. In particular, the persistent rise in variability of total algae, bloom-forming taxa, and cyanotoxins is more consistent with the paradox of enrichment wherein ecological resilience and predictability declined (Cottingham et al., 2000; Bunting et al., 2016; Carpenter et al., 2022).

The rising variability of primary producers probably reflects persistent increases in external forcing (Dakos et al., 2015; Huang et al., 2022) or the constraints of

562 similar large lakes to establish alternative stable states (Scheffer and van Nes, 2007;
563 Janssen et al., 2014; Bruel et al., 2021). Although a series of measures costing
564 ~US$30 billion have been implemented to address wastewater discharge and improve
565 water quality in Lake Taihu watershed (Qin et al., 2019), recent warming climate and
566 extreme weather continue to exacerbate non-point nutrient loading (Xu et al., 2021)
567 and internal release from sediments (Yin et al., 2022). Meanwhile, growing evidence
568 indicates that cyanobacterial dominance is exerting a positive feedback with climate
569 warming (Huisman et al., 2018; Meerhoff et al., 2022), as blooms usually promote the
570 release of nutrients (Xu et al., 2021; Yin et al., 2022) and greenhouse gases (Yan et al.,
571 2017) that increase the warming potential. Under these circumstances, cyanobacterial
572 dominance may thus be a self-perpetuating phenomenon (Havens and Paerl, 2015;
573 Meerhoff et al., 2022), and toxic HABs are predicted to increase continuously in Lake
574 Taihu with climate change. Outside of the littoral habitats and east bays of Lake Taihu,
575 it is arguable that the pelagic areas have always lacked enough macrophytes as a
576 result of strong winds (Zhang et al., 2018b), therefore alternative stable states are
577 unlikely to occur there.

578 It is particularly noteworthy that the synergistic effects of eutrophication and
579 climate change can reduce ecosystem resilience and cause unexpected collapse (e.g.,
580 cyanobacterial HABs), even when individual stressors remain at levels that are
581 considered to be safe (Ryo et al., 2019; Meerhoff et al., 2022). Since long-term
582 eutrophication altered the nutrient cycling and reorganized the configurations of
583 primary producers and food webs in Lake Taihu and beyond, as discussed above, the

584 ecosystems are likely more responsive to warming than before state shift (Fig. 4B).
585 Ecological resistance and vulnerability to climate change thus inherited the legacy of
586 local human pressure similar to previous observations (Battarbee et al., 2005; Bruel et
587 al., 2021). As a consequence, if local pressures (e.g., nutrients) must be reduced to
588 build resilience and mitigate blooms, reduction strategies may be overwhelmed by
589 climate change impacts on the ecosystems, unless more costly and aggressive
590 approaches are employed. Furthermore, the current and future managers should
591 acknowledge that the ecosystem changed permanently to different configurations with
592 shifting baselines beyond the pre-disturbance reference (Fig. 4B) (Battarbee et al.,
593 2005; Ryo et al., 2019). It is important to realize the contemporary process (e.g.,
594 re-oligotrophication), the hysteresis of ecological response (Scheffer et al., 2001), and
595 the integral eutrophication history when setting appropriate eco-environmental
596 baselines. Our study underlines the complexity and interactivity of multiple stressors
597 on lake ecosystems and HABs, and the necessity of long-term perspectives to
598 contextualize modern ecological conditions and inform integrated management.

599 **4.3. Integrated biomarker reconstruction: merits and prospects**

600 In contrast to *in-situ* monitoring and remote sensing observations of lake surface,
601 our novel analysis produces a longer-term, continuous record of lake primary
602 productivity and HABs, which integrates phytoplankton from both surface and deeper
603 waters (McGowan, 2013; Waters et al., 2021). This supplement allows to assess the
604 complete trajectory, magnitude, and decadal variability of ecosystem deterioration,
605 particularly covering a time span where abrupt ecological shifts and toxic HABs occur.

606 The paleo-reconstruction can further shed light on the dynamics of algal community
607 composition, toxin-producing taxa, and toxicity risk of cyanobacterial HABs through
608 time, which may facilitate the development of effective control and restoration
609 strategies.

610 However, specific taxa and biodiversity changes of harmful algae particularly
611 cyanobacteria are still difficult to be determined using biogeochemical tools. The
612 next-generation high-throughput sequencing of environmental DNA is increasingly
613 recognized as an effective complementary means (Domaizon et al., 2017; Monchamp
614 et al., 2018; Zhang et al., 2023). A combined application of molecular biomarkers and
615 DNA techniques to well-dated sediment sequences is thus very promising in
616 deepening our understanding of long-term lake ecosystem dynamics, biodiversity,
617 functioning, and their linkages to environmental forcing. Meanwhile, the
618 spatiotemporal heterogeneity of limnological characteristics, sedimentation, and
619 anthropogenic disturbances in most large lakes like Taihu requires future research
620 with multiple, well-placed cores (Lin et al., 2020, 2021) to improve the assessment of
621 HABs and eco-environmental risk on the whole-lake scale.

622 ## 5. Conclusions

623 We applied molecular biomarkers of aliphatic hydrocarbons, photosynthetic
624 pigments, and cyanotoxins on lake sediment sequences to successfully reconstruct the
625 long-term trajectories and variability of cyanobacterial HABs, which provided
626 empirical evidence on the abrupt regime shifts and causes underlying aquatic

627 ecosystem degradation. The biomarker reconstruction in China's Lake Taihu revealed
628 that significant increases in cyanotoxins lagged behind the initial blooms by over a
629 decade, until the formation of toxic *Microcystis* blooms in the 1990s. This process
630 was accompanied with the shift to and the occurrence of more toxic microcystins
631 (MC-LR and MC-YR), leading to exacerbated harmful effects. Our ordination and
632 numerical modelling results emphasize the synergy of climate warming and
633 eutrophication through nutrient recycling and their feedback through buoyant
634 cyanobacterial proliferation, which sustain bloom-forming potential and promote the
635 occurrence of increasingly-toxic cyanotoxins. Cyanobacterial dominance particularly
636 in shallow lakes may become a self-perpetuating phenomenon, and toxic HAB
637 outbreaks are likely to occur continuously with climate change.

638 The increasing variance and rate of change metrics of phytoplankton
639 (particularly bloom-forming taxa) in Lake Taihu probably indicated increased
640 ecosystem vulnerability and resilience loss with potential risk to shift to another
641 undesirable state. We deduce that an alternative stable state has not yet been
642 established there. Current ecological resistance and vulnerability to climate warming
643 inherited the legacy of local human pressure (e.g., lake eutrophication and alterations
644 of food web), with shifting baseline beyond the pre-disturbance reference. To build
645 resilience and reverse blooms, therefore, more aggressive and integrated strategies
646 dealing with legacy nutrients and global warming are imperative. Taken together, our
647 work provides novel approach and long-term evolutionary perspective for studying
648 the underlying mechanisms triggering HABs with critical insights on water resource

management.

Declaration of competing interest

The authors declare that they have no known competing financial interests or personal relationships that could have appeared to influence the work reported in this paper.

Acknowledgments

We are grateful to Chen Cheng, Jinliang Liu, Jian Cai, Xiaoshuang Sun, Linghan Zeng, Teresa Needham, Yilan Liu, Yuxin Zhu, Weilan Xia, and Yanjie Cai for their assistance during the fieldwork and laboratory analyses. We would also like to thank the editor and three anonymous reviewers for their constructive comments. This study was financially supported by the National Natural Science Foundation of China (42007284, 42111530229), the National Key Research and Development Program of China (2022YFF0801101), the Natural Science Foundation of Jiangsu Province of China (BK20201099), and "Innovative and Entrepreneurial Talent Program" of Jiangsu Province (JSSCBS20211389). The author Qi Lin acknowledges the support of the Youth Scientists Group in Nanjing Institute of Geography and Limnology, Chinese Academy of Sciences (No. 2021NIGLASCJH03).

CRediT authorship contribution statement

Qi Lin: Conceptualization, Investigation, Methodology, Formal analysis, Writing – original draft, Writing – review & editing, Funding acquisition. **Ke Zhang:**

Conceptualization, Data curation, Writing – review & editing, Supervision, Project administration, Funding acquisition. **Suzanne McGowan:** Methodology, Writing – review & editing. **Shixin Huang:** Formal analysis, Writing – review & editing. **Qingju Xue:** Investigation, Methodology, Writing – review & editing. **Eric Capo:** Formal analysis, Writing – review & editing. **Can Zhang:** Methodology, Writing – review & editing. **Cheng Zhao:** Methodology, Writing – review & editing. **Ji Shen:** Conceptualization, Supervision, Project administration.

Appendix A. Supporting information

Supporting information to this article include additional analytical methods (Text S1–S2), tables (Tables S1–S3) and figures (Figs. S1–S9) as noted in the text.

References

Andersen, T., Carstensen, J., Hernandez-Garcia, E., Duarte, C.M., 2009. Ecological thresholds and regime shifts: approaches to identification. Trends Ecol. Evol. 24, 49–57. https://doi.org/10.1016/j.tree.2008.07.014.

Battarbee, R.W., Anderson, N.J., Jeppesen, E., Leavitt, P.R., 2005. Combining palaeolimnological and limnological approaches in assessing lake ecosystem response to nutrient reduction. Freshw. Biol. 50, 1772–1780. https://doi.org/10.1111/j.1365-2427.2005.01427.x.

Bjorndahl, J.A., Gushulak, C.A.C., Mezzini, S., Simpson, G.L., Haig, H.A., Leavitt, P.R., Finlay, K., 2022. Abrupt changes in the physical and biological structure of endorheic upland lakes due to 8-m lake-level variation during the 20th century. Limnol. Oceanogr. 67, 1022–1039. https://doi.org/10.1002/lno.12054.

Bruel, R., Sabatier, P., 2020. serac: A R package for ShortlivEd RAdionuclide chronology of recent sediment cores. J. Environ. Radioact. 225, 106449. https://doi.org/10.1016/j.jenvrad.2020.106449.

693 Bruel, R., Girardclos, S., Marchetto, A., Kremer, K., Crouzet, C., Reyss, J-L., Sabatier,
694 P., Perga, M-E., 2021. Reframing Lake Geneva ecological trajectory in a context
695 of multiple but asynchronous pressures. J. Paleolimnol. 65, 353–368.
696 https://doi.org/10.1007/s10933-021-00176-y.

697 Bunting, L., Leavitt, P.R., Simpson, G.L., Wissel, B., Laird, K.R., Cumming, B.F., St
698 Amand, A., Engstrom, D.R., 2016. Increased variability and sudden ecosystem
699 state change in Lake Winnipeg, Canada, caused by 20th century agriculture.
700 Limnol. Oceanogr. 61, 2090–2107. https://doi.org/10.1002/lno.10355.

701 Cao, X., Xu, X., Bian, R., Wang, Y., Yu, H., Xu, Y., Duan, G., Bi, L., Chen, P., Gao, S.,
702 Wang, J., Peng, J., Qu, J., 2020. Sedimentary ancient DNA metabarcoding
703 delineates the contrastingly temporal change of lake cyanobacterial communities.
704 Water Res. 183, 116077. https://doi.org/10.1016/j.watres.2020.116077.

705 Carey, C.C., Ibelings, B.W., Hoffmann, E.P., Hamilton, D.P., Brookes, J.D., 2012.
706 Eco-physiological adaptations that favour freshwater cyanobacteria in a changing
707 climate. Water Res. 46, 1394–1407. https://doi.org/10.1016/j.watres.2011.12.016.

708 Carpenter, S.R., Arani, B.M.S., Van Nes, E.H., Scheffer, M., Pace, M.L., 2022.
709 Resilience of phytoplankton dynamics to trophic cascades and nutrient
710 enrichment. Limnol. Oceanogr. 67, S258–S265.
711 https://doi.org/10.1002/lno.11913.

712 Carpenter, S.R., Cole, J.J., Pace, M.L., Batt, R., Brock, W.A., Cline, T., Coloso, J.,
713 Hodgson, J.R., Kitchell, J.F., Seekell, D.A., Smith, L., Weidel, B., 2011. Early
714 warnings of regime shifts: a whole-ecosystem experiment. Science 332,
715 1079–1082. https://doi.org/10.1126/science.1203672.

716 Cheng, C., Steinman, A.D., Zhang, K., Lin, Q., Xue, Q., Wang, X., Xie, L., 2023.
717 Risk assessment and identification of factors influencing the historical
718 concentrations of microcystin in Lake Taihu, China. J. Environ. Sci. 127, 1–14.
719 https://doi.org/10.1016/j.jes.2022.03.043.

720 Cottingham, K.L., Rusak, J.A., Leavitt, P.R., 2000. Increased ecosystem variability
721 and reduced predictability following fertilization: Evidence from
722 palaeolimnology. Ecol. Lett. 3, 340–348.
723 https://doi.org/10.1046/j.1461-0248.2000.00158.x.

724 Dakos, V., Carpenter, S.R., van Nes, E.H., Scheffer, M., 2015. Resilience indicators:
725 prospects and limitations for early warnings of regime shifts. Philos. Trans. R.
726 Soc. B Biol. Sci. 370, 20130263. https://doi.org/10.1098/rstb.2013.0263.

727 Deng, J., Qin, B., Paerl, H.W., Zhang, Y., Wu, P., Ma, J., Chen, Y., 2014. Effects of
728 nutrients, temperature and their interactions on spring phytoplankton community
729 succession in Lake Taihu, China. PLoS One 9, e113960.
730 https://doi.org/10.1371/journal.pone.0113960.

731 Domaizon, I., Winegardner, A., Capo, E., Gauthier, J., GregoryEaves, I., 2017.
732 DNA-based methods in paleolimnology: new opportunities for investigating
733 long-term dynamics of lacustrine biodiversity. J. Paleolimnol. 58, 1−21.
734 https://doi.org/10.1007/s10933-017-9958-y.

735 Ellis, E.C., Wang, S., 1997. Sustainable traditional agriculture in the Tai Lake region
736 of China. Agric. Ecosyst. Environ. 61, 177–193.
737 https://doi.org/10.1016/S0167-8809(96)01099-7.

738 Ficken, K.J., Li, B., Swain, D.L., Eglinton, G., 2000. An *n*-alkane proxy for the
739 sedimentary input of submerged/floating freshwater aquatic macrophytes. Org.
740 Geochem. 31, 745–749. https://doi.org/10.1016/S0146-6380(00)00081-4.

741 Guo, C., Zhu, G., Qin, B., Zhang, Y., Zhu, M., Xu, H., Chen, Y., Paerl, H.W., 2019.
742 Climate exerts a greater modulating effect on the phytoplankton community after
743 2007 in eutrophic Lake Taihu, China: Evidence from 25 years of recordings.
744 Ecol. Indic. 105, 82–91. https://doi.org/10.1016/j.ecolind.2019.05.034.

745 Havens, K.E., Paerl, H.W., 2015. Climate change at a crossroad for control of harmful
746 algal blooms. Environ. Sci. Technol. 49, 12605–12606.
747 https://doi.org/10.1021/acs.est.5b03990.

748 Hayes, N.M., Haig, H.A., Simpson, G.L., Leavitt, P.R., 2020. Effects of lake warming
749 on the seasonal risk of toxic cyanobacteria exposure. Limnol. Oceanogr. Lett. 5,
750 393–402. https://doi.org/10.1002/lol2.10164.

751 Henao, E., Rzymski, P., Waters, M.N., 2019. A review of the study of cyanotoxins in
752 paleolimnological research: Current knowledge and future needs. Toxins 12, 6.
753 https://doi.org/10.3390/toxins12010006.

754 Hesse, K., Dittmann, E., Borner, T., 2001. Consequences of impaired microcystin
755 production for light-dependent growth and pigmentation of *Microcystis*
756 *aeruginosa* PCC 7806. FEMS Microbiol. Ecol. 37, 39–43.
757 https://doi.org/10.1016/S0168-6496(01)00142-8.

758 Ho, J.C., Michalak, A.M. Pahlevan, N., 2019. Widespread global increase in intense
759 lake phytoplankton blooms since the 1980s. Nature 574, 667–670.

https://doi.org/10.1038/s41586-019-1648-7.

Hu, L., Shan, K., Lin, L., Shen, W., Huang, L., Gan, N., Song, L., 2016. Multi-year assessment of toxic genotypes and microcystin concentration in northern Lake Taihu, China. Toxins 8, 23. https://doi.org/10.3390/toxins8010023.

Huang, S., Zhang, K., Lin, Q., Kattel, G., Shen, J., 2022. Lake ecosystem regime shifts induced by agricultural intensification: A century scale paleolimnological investigation from the Huai River Basin (China). Quat. Sci. Rev. 285, 107522. https://doi.org/10.1016/j.quascirev.2022.107522.

Huisman, J., Codd, G.A., Paerl, H.W., Ibelings, B.W., Verspagen, J., Visser, P.M., 2018. Cyanobacterial blooms. Nat. Rev. Microbiol. 16, 471–483. https://doi.org/10.1038/s41579-018-0040-1.

Huo, S., Zhang, H., Monchamp, M-E., Wang, R., Weng, N., Zhang, J.B., Zhang, H., Wu, F., 2022. Century-long homogenization of algal communities is accelerated by nutrient enrichment and climate warming in lakes and reservoirs of the North Temperate Zone. Environ. Sci. Technol. 56, 3780–3790. https://doi.org/10.1021/acs.est.1c06958.

Ibrahim, A., Capo, E., Wessels, M., Martin, I., Meyer, A., Schleheck, D., Epp, L.S., 2020. Anthropogenic impact on the historical phytoplankton community of Lake Constance reconstructed by multimarker analysis of sediment-core environmental DNA. Mol. Ecol. 30, 3040–3056. https://doi.org/10.1111/mec.15696.

Janssen, A.B.G., Teurlincx, S., An, S., Janse, J.H., Paerl, H.W., Mooij, W.M., 2014. Alternative stable states in large shallow lakes? J. Great Lakes Res. 40, 813–826. https://doi.org/10.1016/j.jglr.2014.09.019.

Jeppesen, E., Canfield, D.E., Bachmann, R.W., Søndergaard, M., Havens, K.E., Johansson, L.S., Lauridsen, T.L., Sh, T., Rutter, R.P., Warren, G., 2020. Toward predicting climate change effects on lakes: a comparison of 1656 shallow lakes from Florida and Denmark reveals substantial differences in nutrient dynamics, metabolism, trophic structure, and top-down control. Inland Waters. 10, 197–211. https://doi.org/10.1080/20442041.2020.1711681.

Kakouei, K., Kraemer, B.M., Anneville, O., Carvalho, L., Feuchtmayr, H., Graham, J.L., Higgins, S., Pomati, F., Rudstam, L.G., Stockwell, J.D., Thackeray, S.J., 2021. Phytoplankton and cyanobacteria abundances in mid-21st century lakes depend strongly on future land use and climate projections. Glob. Chang. Biol.

27, 6409–6422. https://doi.org/10.1111/gcb.15866.

Kosten, S., Huszar, V.L.M., Becares, E., Costs, L.S., van Donk, E., Hansson, L.A., Jeppesen, E., Kruk, C., Lacerot, G., Mazzeo, N., De Meester, L., Moss, B., Lürling, M., Nõges, T., Romo, S., Scheffer, M., 2012. Warmer climates boost cyanobacterial dominance in shallow lakes. Glob. Chang. Bio. 18, 118–126. https://doi.org/10.1111/j.1365-2486.2011.02488.x.

Leavitt, P.R., 1993. A review of factors that regulate carotenoid and chlorophyll deposition and fossil pigment abundance. J. Paleolimnol. 9, 109–127. https://doi.org/10.1007/BF00677513.

Leavitt, P. R., Vinebrooke, R.D., Donald, D.B., Smol, J.P., Schindler, D.W., 1997. Past ultraviolet radiation environments in lakes derived from fossil pigments. Nature 388, 457–459. https://doi.org/10.1038/41296.

Leavitt, P.R., Fritz, S.C., Anderson, N.J., Baker, P.A., Blenckner, T., Bunting, L., Catalan, J., Conley, D.J., Hobbs, W.O., Jeppesen, E., Korhola, A., McGowan, S., Ruhland, K., Rusak, J.A., Simpson, G.L., Solovieva, N., Werne, J., 2009. Paleolimnological evidence of the effects on lakes of energy and mass transfer from climate and humans. Limnol. Oceanogr. 54, 2330–2348. https://doi.org/10.4319/lo.2009.54.6_part_2.2330.

Lin, Q., Zhang, K., Liu, E., Sabatier, P., Arnaud, F., Shen, J., 2020. Deciphering centurial anthropogenic pollution processes in large lakes dominated by socio-economic impacts. Anthropocene 32, 100269. https://doi.org/10.1016/j.ancene.2020.100269.

Lin, Q., Zhang, K., McGowan, S., Capo, E., Shen, J., 2021. Synergistic impacts of nutrient enrichment and climate change on long-term water quality and ecological dynamics in contrasting shallow-lake zones. Limnol. Oceanogr. 66, 3271–3286. https://doi.org/10.1002/lno.11878.

Lürling, M., van Oosterhout, F., de Senerpont Domis, L., Marinho, M.M., 2018. Response of natural cyanobacteria and algae assemblages to a nutrient pulse and elevated temperature. Front. Microbiol. 9, 1851. https://doi.org/10.3389/fmicb.2018.01851.

Mao, Z., Gu, X., Cao, Y., Zhang, M., Zeng, Q., Chen, H., Shen, R., Jeppesen, E., 2020. The role of top-down and bottom-up control for phytoplankton in a subtropical shallow eutrophic lake: Evidence based on long-term monitoring and modeling. Ecosystems 23, 1449–1463. https://doi.org/10.1007/s10021-020-00480-0.

McGowan, S., 2013. Pigment studies. In: Elias, S. (Ed.), Encyclopedia of Quaternary Sciences. Elsevier, pp. 1–26. https://doi.org/10.1016/b0-444-52747-8/00247-7.

McGowan, S., Barker, P., Haworth, E.Y., Leavitt, P.R., Maberly, S.C., Pates, J., 2012. Humans and climate as drivers of algal community change in Windermere since 1850. Freshw. Biol. 57, 260–277. https://doi.org/10.1111/j.1365-2427.2011.02689.x.

Meerhoff, M., Audet, J., Davidson, T.A., De Meester, L., Hilt, S., Kosten, S., Liu, Z., Mazzeo, N., Paerl, H.W., Scheffer, M., Jeppesen, E., 2022. Feedback between climate change and eutrophication: revisiting the allied attack concept and how to strike back. Inland Waters 12, 187–204. https://doi.org/10.1080/20442041.2022.2029317.

Meyers, P.A., 2003. Applications of organic geochemistry to paleolimnological reconstructions: a summary of examples from the Laurentian Great Lakes. Org. Geochem. 34, 261–289. https://doi.org/10.1016/S0146-6380(02)00168-7.

Monchamp, M.E., Spaak, P., Domaizon, I., Dubois, N., Bouffard, D., Pomati, F., 2018. Homogenization of lake cyanobacterial communities over a century of climate change and eutrophication. Nat. Ecol. Evol. 2, 317–324. https://doi.org/10.1038/s41559-017-0407-0.

Moss, B., Kosten, S., Meerhoff, M., Battarbee, R.W., Jeppesen, E., Mazzeo, N., Havens, K., Lacerot, G., Liu, Z., De Meester, L., Paerl, H.W., Scheffer, M., 2011. Allied attack: climate change and eutrophication. Inland Waters 1, 101–105. https://doi.org/10.5268/IW-1.2.359.

Paerl, H.W., Scott, J.T., 2010. Throwing fuel on the fire: synergistic effects of excessive nitrogen inputs and global warming on harmful algal blooms. Environ. Sci. Technol. 44, 7756–7758. https://doi.org/10.1021/es102665e.

Perga, M-E., Frossard, V., Jenny, J-P., Alric, B., Arnaud, F., Berthon, V., Black, J.L., Domaizon, I., Giguet-Covex, C., Kirkham, A., Magny, M., Manca, M., Marchetto, A., Millet, L., Pailleś, C., Pignol, C., Poulenard, J., Reyss, J-L., Rimet, F., Sabatier, P., Savichtcheva, O., Sylvestre, F., Verneaux, V., 2015. High-resolution paleolimnology opens new management perspectives for lakes adaptation to climate warming. Front. Ecol. Environ. 3, 1–17. https://doi.org/10.3389/fevo.2015.00072.

Qin, B., Paerl, H.W., Brookes, J.D., Liu, J.Q., Jeppesen, E., Zhu, G., Zhang, Y., Xu, H., Shi, K., Deng, J., 2019. Why Lake Taihu continues to be plagued with

cyanobacterial blooms through 10 years (2007–2017) efforts. Sci. Bull. 64, 354–356. https://doi.org/10.1016/j.scib.2019.02.008.

Richardson, J., Feuchtmayr, L., Miller, C., Hunter, P.D., Maberly, S.C., Carvalho, L., 2019. Response of cyanobacteria and phytoplankton abundance to warming, extreme rainfall events and nutrient enrichment. Glob. Chang. Biol. 25, 3365–3380. https://doi.org/10.1111/gcb.14701.

Ryo, M., Aguilar-Trigueros, C.A., Pinek, L., Muller, L.A.H., Rillig, M.C., 2019. Basic principles of temporal dynamics. Trends Ecol. Evol. 34, 723 – 733. https://doi.org/10.1016/j.tree.2019.03.007.

Scheffer, M., Carpenter, S., Foley, J.A., Folke, C., Walker, B., 2001. Catastrophic shifts in ecosystems. Nature 413, 591–596. https://doi.org/10.1038/35098000

Scheffer, M., van Nes, E.H., 2007. Shallow lakes theory revisited: Various alternative regimes driven by climate, nutrients, depth and lake size. Hydrobiologia 585, 455–466. https://doi.org/10.1007/s10750-007-0616-7.

Shi, K., Zhang, Y., Zhang, Y., Li, N., Qin, B., Zhu, G., Zhou, Y., 2019. Phenology of phytoplankton blooms in a trophic lake observed from long-term MODIS data. Environ. Sci. Technol. 53, 2324–2331. https://doi.org/10.1021/acs.est.8b06887.

Smol, J.P., 2010. The power of the past: using sediments to track the effects of multiple stressors on lake ecosystems. Freshw. Biol. 55, 43–59. https://doi.org/10.1111/j.1365-2427.2009.02373.x.

Simpson, G.L. 2018. Modelling palaeoecological time series using generalised additive models. Front. Ecol. Evol. 6, 149. https://doi.org/10.3389/fevo.2018.00149.

Taranu, Z.E., Gregory-Eaves, I., Leavitt, P.R., Bunting, L., Buchaca, T., Catalan, J., Domaizon, I., Guilizzoni, P., Lami, A., McGowan, S., Moorhouse, H., Morabito, G., Pick, F.R., Stevenson, M.A., Thompson, P.L., Vinebrooke, R.D., 2015. Acceleration of cyanobacterial dominance in north temperate-subarctic lakes during the Anthropocene. Ecol. Lett. 18, 375–384. https://doi.org/10.1111/ele.12420.

Taranu, Z.E., Gregory-Eaves, I., Steele, R., Beaulieu, M., Legendre, P., 2017. Predicting microcystin occurrences in US lakes and reservoirs: A new framework for modeling the drivers of an important health risk factor. Glob. Ecol. Biogeog. 26, 625–637. https://doi.org/10.1111/geb.12569.

Taranu, Z.E., Pick, F.R., Creed, I.F., Zastepa, A., Watson, S.B., 2019. Meteorological and nutrient conditions influence microcystin congeners in freshwaters. Toxins 11, 620. https://doi.org/10.3390/toxins11110620.

ter Braak, C.J.F., Šmilauer., P., 2012. CANOCO reference manual and user's guide: Software for ordination (version 5.0). Microcomputer Power.

Waters, M.N., Brenner, M., Curtis, J.H., Romero-Oliva, C.S., Dix, M., Cano, M., 2021. Harmful algal blooms and cyanotoxins in Lake Amatitlán, Guatemala, coincided with ancient Maya occupation in the watershed. Proc. Natl. Acad. Sci. U. S. A. 118, e2109919118. https://doi.org/10.1073/pnas.2109919118.

Wood, S.N. (2017). Generalized additive models: An introduction with R (2). Chapman and Hall/CRC Press.

Woolway, R.I., Kraemer, B.M., Lenters, J.D., Merchant, C.J., O'Reilly, C.M., Sharma, S., 2020. Global lake responses to climate change. Nat. Rev. Earth & Environ. 1, 388–403. https://doi.org/10.1038/s43017-020-0067-5.

Xu, H., McCarthy, M.J., Paerl, H. W., Brookes, J.D., Zhu, G., Hall, N.S., Qin, B., Zhang, Y., Zhu, M., Hampel, J.J., Newell, S.E., Gardner, W.S., 2021. Contributions of external nutrient loading and internal cycling to cyanobacterial bloom dynamics in Lake Taihu, China: Implications for nutrient management. Limnol. Oceanogr. 66, 1492–1509. https://doi.org/10.1002/lno.11700.

Xue, Q., Xie, L., Cheng, C., Su, X., Zhao, Y., 2023. Different environmental factors drive the concentrations of microcystin in particulates, dissolved water, and sediments peaked at different times in a large shallow lake. J. Environ. Manag. 326, 116833. https://doi.org/10.1016/j.jenvman.2022.116833

Yan, X., Xu, X., Wang, M., Wang, G., Wu, S., Li, Z., Sun, H., Shi, A., Yang, Y., 2017. Climate warming and cyanobacteria blooms: looks at their relationships from a new perspective. Water Res. 125, 449 – 457. https://doi.org/10.1016/j.watres.2017.09.008.

Yang, J., Lv, H., Isabwe, A., Liu, L., Yu, X., Chen, H., Yang, J., 2017. Disturbance-induced phytoplankton regime shifts and recovery of cyanobacteria dominance in two subtropical reservoirs. Water Res. 120, 52–63. https://doi.org/10.1016/j.watres.2017.04.062.

Yang, Z., Zhang, M., Shi, X., Kong, F., Ma, R., Yu, Y., 2016. Nutrient reduction magnifies the impact of extreme weather on cyanobacterial bloom formation in

large shallow Lake Taihu (China). Water Res. 103, 302–310. https://doi.org/10.1016/j.watres.2016.07.047.

Yin, H., Zhang, M., Yin, P., Li, J., 2022. Characterization of internal phosphorus loading in the sediment of a large eutrophic lake (Lake Taihu, China). Water Res. 225, 119125. https://doi.org/10.1016/j.watres.2022.119125.

Zastepa, A., Taranu, Z.E., Kimpe, L.E., Blais, J.M., Gregory-Eaves, I., Zurawell, R.W., Pick, F.R., 2017. Reconstructing a long-term record of microcystins from the analysis of lake sediments. Sci. Total Environ. 579, 893–901. https://doi.org/10.1016/j.scitotenv.2016.10.211.

Zeng, L., Swann, G.E.A., Leng, M.J., Chen, X., Ji, J., Huang, X., McGowan, S., 2023. Ecosystem deterioration in the middle Yangtze floodplain lakes over the last two centuries: Evidence from sedimentary pigments. Quat. Sci. Rev. 302, 107954. https://doi.org/10.1016/j.quascirev.2023.107954.

Zhang, C., Zhao, C., Zhou, A., Zhang, K., Wang, R., Shen, J., 2019. Late Holocene lacustrine environmental and ecological changes caused by anthropogenic activities in the Chinese Loess Plateau. Quat. Sci. Rev. 203, 266–277. https://doi.org/10.1016/j.quascirev.2018.11.020.

Zhang, J., Shi, K., Paerl, H.W., Rühland, K.M., Yuan, Y., Wang, R., Chen, J., Ge, M., Zheng, L., Zhang, Z., Qin, B., Liu, J., Smol, J.P., 2023. Ancient DNA reveals potentially toxic cyanobacteria increasing with climate change. Water Res. 229, 119435. https://doi.org/10.1016/j.watres.2022.119435.

Zhang, M., Shi, X., Yang, Z., Yu, Y., Shi, L., Qin, B., 2018a. Long-term dynamics and drivers of phytoplankton biomass in eutrophic Lake Taihu. Sci. Total Environ. 645, 876–886. https://doi.org/10.1016/j.scitotenv.2018.07.220.

Zhang, Y., Qin, B., Zhu, G., Shi, K., Zhou, Y., 2018b. Profound changes in the physical environment of Lake Taihu from 25 years of long-term observations: implications for algal bloom outbreaks and aquatic macrophyte loss. Water Resour. Res. 54, 4319–4331. https://doi.org/10.1029/2017WR022401.

Zhang, Y., Su, Y., Liu, Z., Yu, J., Jin, M., 2017. Lipid biomarker evidence for determining the origin and distribution of organic matter in surface sediments of Lake Taihu, eastern China. Ecol. Indic. 77, 397–408. https://doi.org/10.1016/j.ecolind.2017.02.031.

Zhou, J., Leavitt, P.R., Zhang, Y.B., Qin, B.Q., 2022. Anthropogenic eutrophication of

shallow lakes: Is it occasional? Water Res. 221, 118728. https://doi.org/10.1016/j.watres.2022.118728.

Zhu, L., Shi, W., Van Dam, B., Kong, L., Yu, J., Qin, B., 2020. Algal accumulation decreases sediment nitrogen removal by uncoupling nitrification-denitrification in shallow eutrophic lakes. Environ. Sci. Technol. 2020, 54, 6194–6201. https://doi.org/10.1021/acs.est.9b05549.

Zhu, M., Paerl, H.W., Zhu, G., Wu, T., Li, W., Shi, K., Zhao, L., Zhang, Y., Qin, B., Caruso, A.M., 2014. The role of tropical cyclones in stimulating cyanobacterial (*Microcystis* spp.) blooms in hypertrophic Lake Taihu, China. Harmful Algae 39, 310–321. https://doi.org/10.1016/j.hal.2014.09.003.

Graphical Abstract

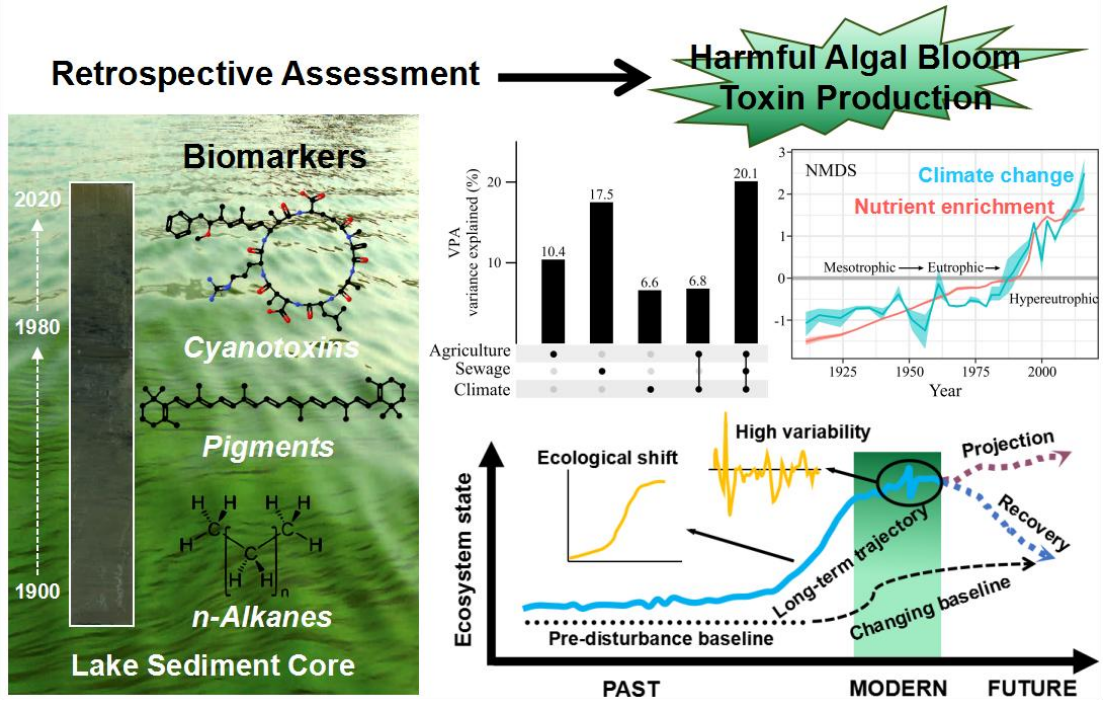

Figures

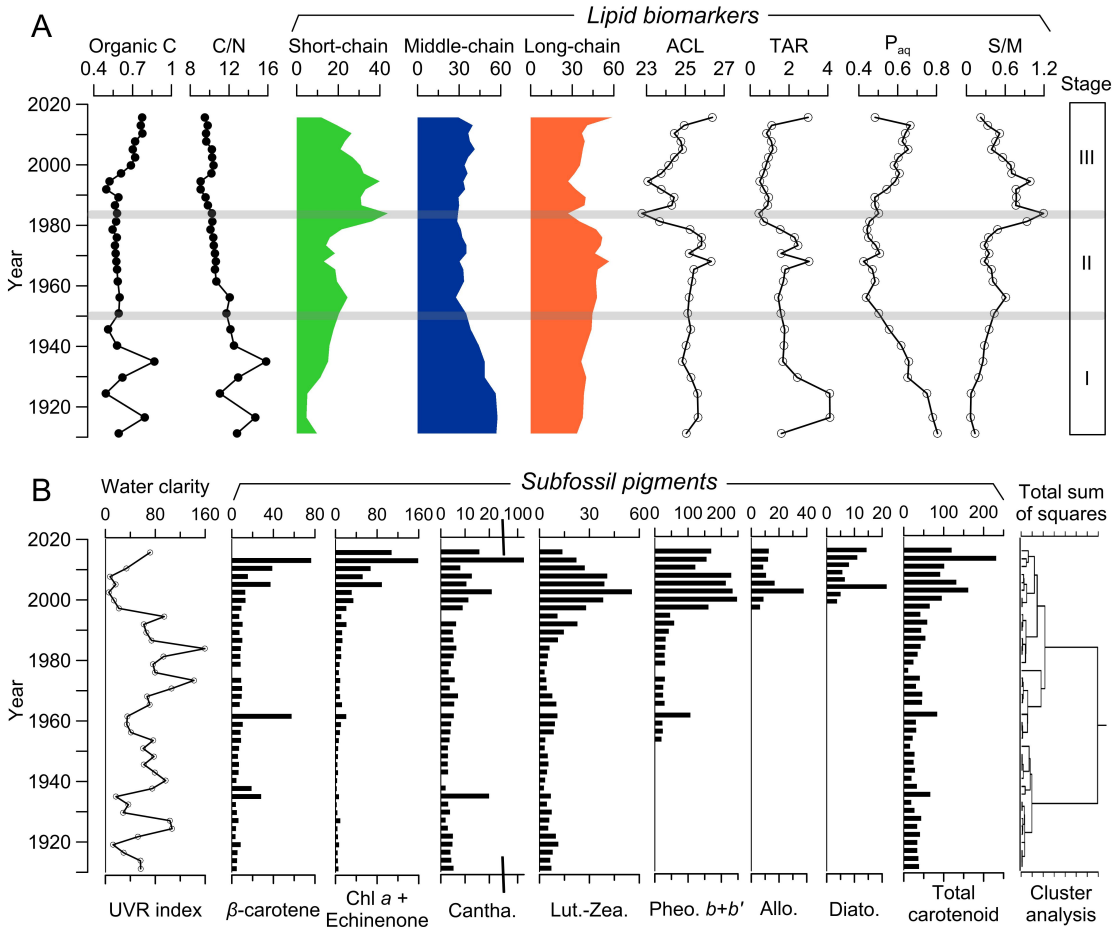

Fig. 1. Temporal changes of lipid and subfossil pigment biomarkers in Lake Taihu sediment cores. (A) Profiles of sedimentary organic C (%), molar ratios of C/N, total *n*-alkanes within different length of chains (%), and selected *n*-alkane proxies (ACL, TAR, P_{aq}, and S/M) (Text S1). The grey horizontal bars partition three potential change phases for lipid biomarkers. (B) Profiles of sedimentary chlorophyll and carotenoid pigments (nmol g^{-1} OC) and UVR index along with the CONISS cluster analysis. Cantha. = canthaxanthin (colonial cyanobacteria), Lut.-Zea. = lutein-zeaxanthin (chlorophytes and cyanobacteria pigments, i.e., "bloom-forming" taxa), Pheo. *b*+*b*′ = pheophytin *b*+*b*′ (chlorophytes), Allo. = alloxanthin

(cryptophytes), Diato. = diatoxanthin (primarily diatoms), Chl *a* + Echinenone (all phototrophs and total cyanobacteria), and β-carotene or total carotenoid (total autotrophic production).

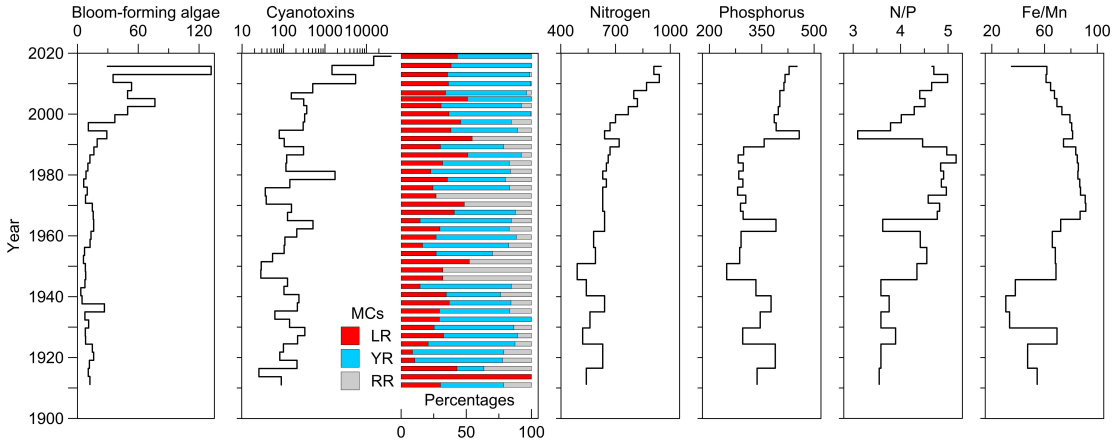

Fig. 2. Historical reconstruction of harmful algal blooms and cyanotoxin production associated with sedimentary nutrient and redox variables in Lake Taihu. Bloom-forming algae is indicated by the sum of canthaxanthin and lutein-zeaxanthin pigments (nmol g^{-1} OC). Cyanotoxins are reported as the sum of three dominant microcystin congeners (MC-LR, MC-YR, MC-RR) (ng g^{-1} OC) and their relative percentages. Total sediment nitrogen (mg kg^{-1}), phosphorus (mg kg^{-1}), and molar ratios of N/P and Fe/Mn are also shown.

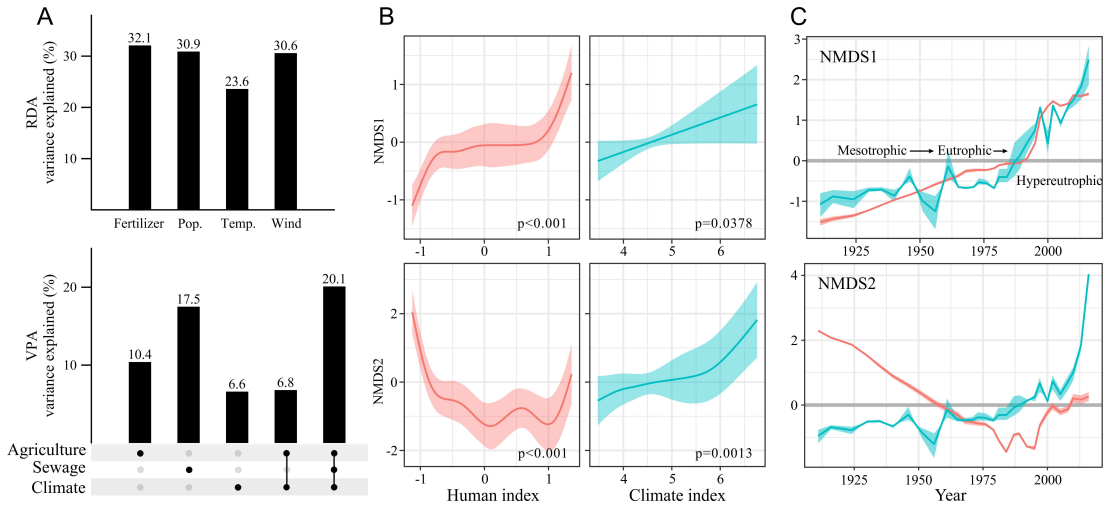

Fig. 3. Multivariate statistical analysis illustrating the dynamic relationships between paleorecords and forward selected environmental variables. (A) Century-long variation in gecochemical variables and multi-biomarkers explained by categories of agriculture (fertilizer consumption), sewage (population), climate (air temperature, wind speed) via four individual runs of redundancy analysis (RDA) and one run of variance partitioning analysis (VPA) (Fig. S9). All categories of significant environmental variables and their interactions are included in VPA. (B) Generalized additive model (GAM) analysis of the fitted smooth functions between the inferred human index, climate index, and scores of both NMDS axes of paleorecords (NMDS1, NMDS2) (Fig. S7). (C) GAM results indicating the contributions (curves with 95% pointwise confidence intervals) of human (red) and climate (blue) variables to NMDS1 and NMDS2 through time. The relative importance of each predictor (increase/decrease) is deduced from the centered-scaled values on y-axis scale except zero, and significant correlations with predictors are shown for each response variable in Table S2.

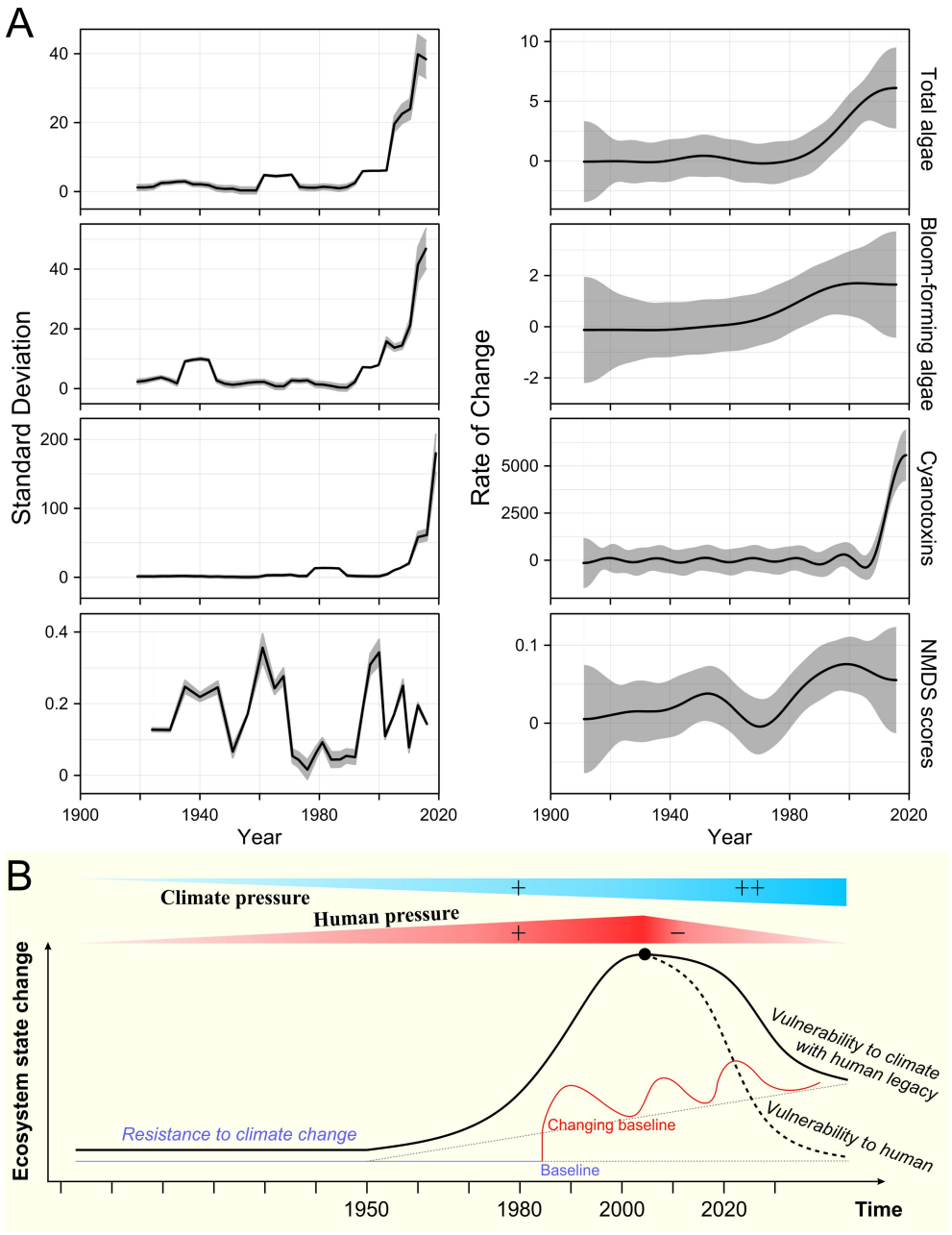

1013

1014 **Fig. 4. Temporal changes in ecological variability and conceptual diagram**
1015 **illustrating the response of Lake Taihu ecosystem to multiple changing stressors**
1016 **through time.** (A) Lake ecosystem variability inferred from variance (standard
1017 deviation, left) and RoC (rate of change, right) metrics of time series of total
1018 autotrophic production (Chl *a* + echinenone), bloom-forming algal abundance (sum of
1019 canthaxanthin and lutein-zeaxanthin), cyanotoxins (total MCs), and the scores of
1020 NMDS1 axis. The gray ribbons are 95% pointwise confidence intervals on the fitted

1021 models. Where the simulation value does not include zero, the models detect increase
1022 or decrease in the ecological variability. (B) Under multiple interactive stressors, the
1023 ecosystem changed through time to different configurations with shifting baseline
1024 beyond pre-disturbance reference (Battarbee et al., 2005; Ryo et al., 2019), and
1025 ecological vulnerability to climate change inherited the human legacy (e.g.,
1026 anthropogenic eutrophication and alterations of food web) with lower resilience.